

## Acknowledgments

This work was supported by NASA Langley Research Center Grant NCC-1-167 and by Air Force Office of Scientific Research Grant F49620-00-1-0074. The authors are extremely grateful to Steven Wilkinson at NASA Langley Research Center for his unlimited help and expertise in conducting this work. We are also grateful to William Sellers, also at NASA Langley Research Center, for his help in coordinating the use of the NASA tunnels.

## References

- <sup>1</sup>Kosinov, A., Maslov, A., and Shevelkov, S., "Experiments on the Stability of Supersonic Laminar Boundary Layers," *Journal of Fluid Mechanics*, Vol. 219, 1990, p. 621.
- <sup>2</sup>Wilkinson, S. P., Anders, S. G., Chen, F. J., and Beckwith, I. E., "Supersonic and Hypersonic Quiet Tunnel Technology at NASA Langley," AIAA Paper 92-3908, 1992.
- <sup>3</sup>Corke, T. C., and Mangano, R. A., "Resonant Growth of Three-Dimensional Modes in Transitioning Blasius Boundary Layers," *Journal of Fluid Mechanics*, Vol. 209, 1989, pp. 93-150.
- <sup>4</sup>Corke, T. C., and Kusek, S. M., "Resonance in Axisymmetric Jets with Controlled Helical-Mode Input," *Journal of Fluid Mechanics*, Vol. 249, 1993, pp. 307-336.
- <sup>5</sup>Cavalieri, D. A., "On the Experimental Design for Instability Analysis on a Cone at Mach 3.5 and 6 Using a Corona Discharge Perturbation Method," M.S. Thesis, Mechanical and Aerospace Engineering Dept., Illinois Inst. of Technology, Chicago, Aug. 1995.
- <sup>6</sup>Ng, L. L., and Zang, T. A., "Secondary Instability Mechanisms in Compressible, Axisymmetric Boundary Layers," AIAA Paper 92-0743, 1992.

J. C. Hermanson  
Associate Editor

# Influence of Spike Shape at Supersonic Flow Past Blunt-Nosed Bodies: Experimental Study

Snežana S. Milićević\* and Miloš D. Pavlović†  
University of Belgrade, 11000 Belgrade, Serbia, Yugoslavia

## Introduction

**B**ECAUSE of the appearance of a strong shock wave at a supersonic flight of a projectile, which considerably increases the drag and aerodynamic heating during the projectile's flight through the air, a spike is mounted on its nose to reduce this effect.<sup>1-6</sup> In this way, the strong shock wave is replaced with a system of conical waves, so that the driving force, and consequently the fuel consumption, is reduced. A spike mounted on a blunt body during its flight at an angle of attack decreases the drag and also increases the lift. Therefore, all aircraft at supersonic speeds, such as planes, blunt reentry vehicles, rockets, missiles, etc., are usually spike nosed. Even better effects can be attained using such a simple geometrical construction than in the case of sophistically shaped front side of bodies flying supersonically. However, the applicability of the spike is limited due to the possible appearance of oscillations, which may reduce its positive effects and may cause aerodynamic disturbances during the flight.<sup>1-6</sup>

Many researchers focused their attention predominantly on the influence of the spike's length on the aerodynamic characteristics

of blunt bodies, for various angles of attack at some transonic,<sup>1</sup> supersonic,<sup>2-5</sup> or even hypersonic<sup>2,6</sup> speeds. However, one might question whether the shape of a spike could affect the fluid flow structure and the aerodynamic characteristics of a blunt body. However, this influence has not been systematically analyzed so far. This Note is a contribution to the study of this effect.

This Note presents the results of an experiment that analyzed the influence of the spike's shape on the drag coefficient and the lift coefficient at supersonic flow past blunt-nosed bodies. The experiment was carried out in a wind tunnel, for one value of Mach and Reynolds numbers and for different angles of attack. The aerodynamic forces for the body without a spike and with four different spike shapes were measured. The Note also proposes a criterion for estimating the aerodynamic effect of the spike shape, by using only the schlieren visualization of the flow. The best spike shape from the experimental set of spikes was selected using this qualitative criterion. This selection coincided with the spike selected by the measurement of the aerodynamic coefficient.

The Note briefly reports the results of the research. An in-depth description of the experiment conditions and results may be found in Ref. 5.

## Geometric Characteristics and Experimental Conditions

The geometry of the tested model without and with four different types of spikes<sup>5</sup> is shown in the inset of Fig. 1. The model had a cylindrical body of diameter  $d = 27$  mm, with length  $L = 4.44d$ . Its nose was hemispherical, and its tail was conical, with a semi-angle of 9 deg and with a basis diameter  $d_b = 0.85d$ . All four of the spikes were of the same length  $l = d$ . The first spike (spike 1) had a cylindrical body with a conical nose with the angle of 20 deg. The second (spike 2) and third (spike 3) spikes were conical with the angles of 5 and 10 deg, respectively. The tips of all of these spikes were rounded. The fourth spike (spike 4) had a hemispherical nose and a cylindrical body. All four spikes, as well as the model, were made of steel and finished with high surface quality.

The experiments were carried out in the wind tunnel T-36 in the Technical Institute of the Yugoslav Army. T-36 is a small transonic open wind tunnel with interrupted action. The tunnel test section had a cross section  $0.25 \times 0.25$  m and was 0.6 m long. A classic Tepler system, specially designed to meet high quality and accuracy requirements, was used as the schlieren system for visualization of the fluid flowfield.

The dynamic pressure of undisturbed flow  $q$  was taken as the reference value of pressure, the reference area  $A$  was the cross-sectional area of the cylindrical body of the model, and the reference

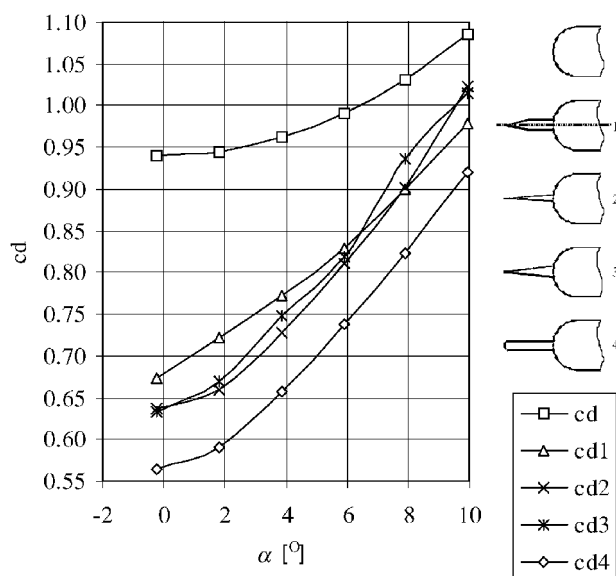


Fig. 1 Relation between the drag coefficient and the angle of attack for the body without ( $c_d$ ) and with the four analyzed spikes ( $c_{d1-4}$ ).

Received 21 June 2001; revision received 28 January 2002; accepted for publication 29 January 2002. Copyright © 2002 by the American Institute of Aeronautics and Astronautics, Inc. All rights reserved. Copies of this paper may be made for personal or internal use, on condition that the copier pay the \$10.00 per-copy fee to the Copyright Clearance Center, Inc., 222 Rosewood Drive, Danvers, MA 01923; include the code 0001-1452/02 \$10.00 in correspondence with the CCC.

\*Teaching Assistant, Faculty of Mechanical Engineering, 27 marta 80; smilicev@rcub.bg.ac.yu.

†Professor, Faculty of Mechanical Engineering, 27 marta 80.

length was its diameter  $d$ . During the experiments, two cycles of measurements were performed. First, the drag coefficients  $c_d$  and the lift coefficients  $c_l$  were calculated from the measured values of the normal and tangential forces for the model without spike and for models with four different types of spikes.<sup>5</sup> The coefficients were based on the forces acting on the entire model, and its estimated<sup>5</sup> accuracy is 0.035. Second, the fluid flowfield around the models was visualized using the schlieren method. All of the experiments were carried out at supersonic flow with Mach number  $M = 1.89$ , Reynolds number  $Re_d = 0.38 \times 10^6$ , and angle of attack  $\alpha$  from  $-4$  to  $10$  deg, with a 2-deg step.

The duration of each measurement was about 20 s. The fluid velocity  $v$ , density  $\rho$ , Mach number  $M$ , dynamic pressure  $q$ , and dynamic viscosity were calculated on the basis of the measured values of stagnation pressure  $p_0$ , stagnation temperature  $T_0$ , static pressure  $p$ , and static temperature  $T$ . The measured and calculated mean values of undisturbed flow were almost the same for all of the experiments: settling chamber  $p_0 = 0.992$  bar and  $T_0 = 278$  K and test section  $p = 0.151$  bar,  $T = 162$  K,  $\rho = 0.324$  kg/m<sup>3</sup>,  $\mu = 0.1097$  Pa · s,  $q = 0.376$  bar,  $v = 482.1$  m/s,  $M = 1.89$ , and  $Re_d = 0.38 \times 10^6$ .

### Results Analysis

It can be clearly seen from Figs. 1 and 2 that both the drag coefficient  $c_d$  and the lift coefficient  $c_l$  increase with the angle of attack  $\alpha$  for all four tested configurations with spikes, as well as for the body without a spike. When a spike is mounted on the nose of a hemispherical-nosed body, a significant reduction of the drag coefficient  $c_d$  occurs, as shown in Fig. 1, along with an increase in the lift coefficient  $c_l$  (Fig. 2). This coincides with other researchers' results.<sup>2,3</sup> However, Figs. 1 and 2 show also another issue, that is, the influence of the spike shape.

The influence of the spike itself and its shape to the drag coefficient value is most notable for the angle of attack near to zero. In that case, note that the drag coefficient value for the model with the first spike was reduced by about 28%, compared to the model without a spike. When the second and third spikes were mounted, the drag coefficient was reduced by about 32%, and the greatest reduction (about 40%) was obtained with the fourth spike. When the angle of attack increases, the relative drag coefficient reduction decreases. At  $\alpha \approx 10$  deg, that reduction for the model with the first spike was about 10%, with the second 6%, with the third 7%, and finally with the fourth 15%. For the range of the tested values of the angle of attack  $\alpha$ , it seems that the fourth spike, with a cylindrical body and a hemispherical nose, is most effective for reduction of the drag coefficient.

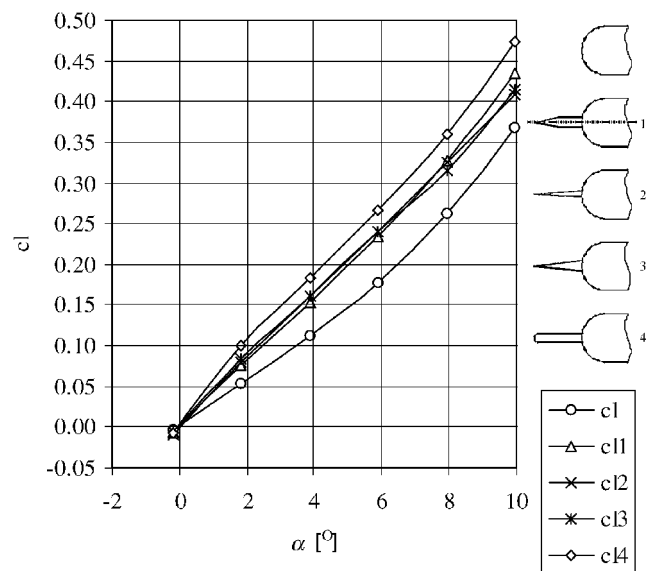


Fig. 2 Relation between the lift coefficient and the angle of attack for the body without (c<sub>l</sub>) and with the four analyzed spikes (c<sub>l1</sub>–4).

It is also clear from Fig. 2 that spike 4 gives the greatest increase of the lift coefficient compared to the model without a spike. The maximum influence on the lift coefficient's increase for all four tested models with spike was obtained for the lowest tested value,  $\alpha \approx 2$  deg. It was 43% for the model with the first spike, 50% with the second spike, 59% with the third spike, and 86% with the fourth spike. That increase of the lift coefficient compared to the model without a spike at  $\alpha \approx 10$  deg for the model with spike 1 was about 18%, with spike 2 about 11%, with the spike 3 13%, and finally with spike 4 29%. To conclude, for the fourth spike (cylindrical shape with a hemispherical tip), the drag force has minimal values and the lift force has maximum values of all of the tested cases, for all tested angles of attack.

Because of the optical adjustment of the schlieren system used, the obtained photographs, even for the angle of attack 0 deg, are asymmetric. The schlieren photographs of the model without a spike,<sup>5</sup> obtained for all of the angles of attack show the front of the shock wave for  $a \approx 0.2d$  ahead the stagnation point. As it distances the body, the wave becomes weaker, and its angle decreases. At the distance of one diameter from the body, this angle is reduced to 45 deg. Behind the shock wave, in the region near the shoulder of the body at the end of the hemispherical nose, an expansion wave can be seen, with expansion lines from 55 to 50.5 deg. There is also another expansion wave, with expansion lines from 44 to 35 deg, at the beginning of the conical tail of the body.

Schlieren photographs of the model with the four different types of spikes are presented in Fig. 3, for the near-zero angle of attack. A strong influence of the spike on the fluid flowfield structure is evident in all four cases. Foremost, a conical shock wave is formed at the tip of the spike. High pressure behind the shock wave provokes boundary-layer separation. An approximately cone-shaped recirculation zone (dead air region) is formed between the wave and the spike, due to the separation. There is a strong deflection of the external flow in the region of the boundary-layer reattachment (on the hemispherical tip of the model), which provokes the appearance of a detached shock wave. As a result of the interaction of this wave with the conical shock wave emanating from the tip, a new, almost conical shock wave is formed. The remainder of the flowfield pattern is the same as for the body without a spike.

The differences between the corresponding characteristic shock angles, for various types of spike, are insignificant. However, the principal difference that can be noted is the joint place of the leading conical shock wave, which is formed on the tip of the spike, and the detached shock wave, formed in the region of the boundary-layer reattachment. For spike 1, this place is the nearest to the axis ( $R_1 \approx 1.1d$ ); for spikes 2 and 3, it is  $R_{2,3} \approx 1.5d$ ; and for spike 4,

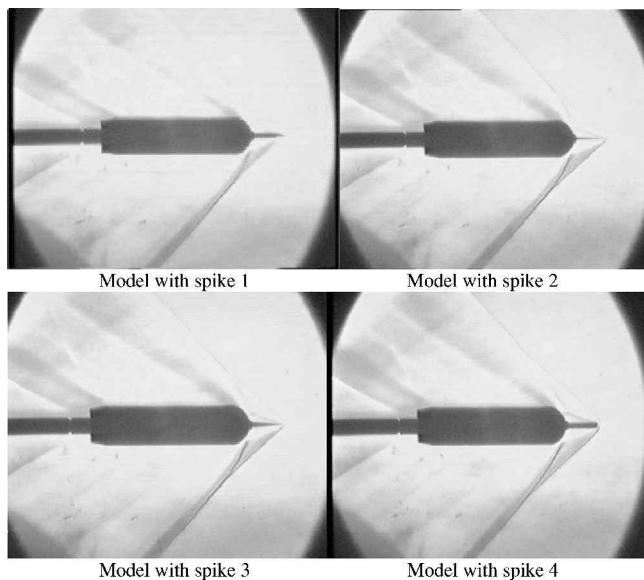


Fig. 3 Schlieren photographs of the model with the four analyzed spikes at near-zero angle of attack.

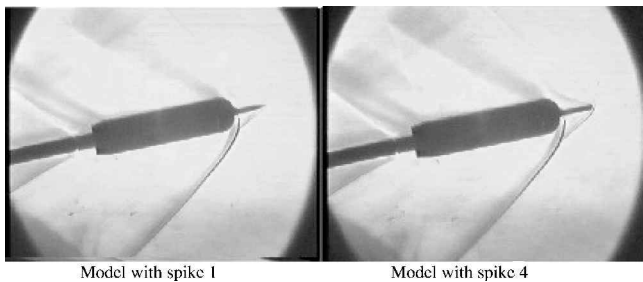


Fig. 4 Schlieren photographs of the model with spikes 1 and 4, at angle of attack  $\alpha \approx 10$  deg.

it is  $R_4 \approx 2d$ . These differences can be explained by the following reasoning. In front of spike 4, with a hemispherical tip, the separated curved shock wave is stronger than the conical shock waves for the other three spikes with conical tips. The angle of that shock wave is  $\beta \approx 45$  deg, when the distance from the axis varies from  $0.1d$  to  $0.5d$ , and decreases to the minimal value  $\beta \approx 43$  deg at the vicinity of its joint point with the secondary (detached) shock wave. For spike 1, the minimal value of that angle is  $\beta \approx 39$  deg and for spikes 2 and 3, the minimal value is  $\beta \approx 42$  deg. The stronger shock wave at the tip of spike 4 is followed by the weaker detached shock wave at the shoulder of the model, which is in a good agreement with the accomplished aerodynamic coefficient analysis.

It appears that the position of the joint point of the leading and the secondary shock wave, obtained by the visualization, is a simple but reliable criterion of the aerodynamic effect of a spike. The greater radial distance of the joint point from the axis indicates the better aerodynamic characteristics (less drag and greater lift) of the tested configuration.

The observed differences among different types of spikes decrease for higher angles of attack, which corresponds well to the results of aerodynamic coefficients, presented in Figs. 1 and 2. The schlieren photographs are given in Fig. 4 for two cases, the model with spike 1 and with the best spike, spike 4, for angle of attack  $\alpha \approx 10$  deg. The distance of the joint point from the axis decreases with ascending the angle of attack  $\alpha$ . This distance measured in the vertical plane, below the axis, is about  $0.5d$  for the model with spike 1 and about  $0.8d$  for the model with spike 4. When it is assumed that this distance represents the criterion, it seems that, even for high values of the angle of attack, spike 4 retains the best aerodynamic characteristics.

The general characteristics of the flow patterns presented in Figs. 3 and 4 are in accordance with the results of other authors.<sup>2,3</sup> No oscillations were noticed for any tested model, which is the same result as for all hemispherical tipped models with spikes.<sup>2-6</sup> Also, because the semi-angle of the recirculation zone for the model with spikes 2 and 3 is about 20 deg (slightly smaller for spike 1 and slightly greater for spike 4), the observed conical shock angles  $\beta$  correspond well to the angle of the conical shock wave that is formed in a supersonic flow ( $M = 1.9$ ) past a cone body with the semi-angle  $\gamma = 20$  deg (Ref. 7).

To validate the obtained results for the lift coefficient, they were compared with the results of Hunt (see Ref. 2) for supersonic flow at  $M = 1.89$ . His spike had a conical tip. For comparison purposes, our results were corrected to reduce the base drag.<sup>5</sup> A good agreement with Hunt's results (see Ref. 2) was obtained for the models with spikes, particularly for spikes 1-3, whereas our results for the best spike, spike 4, were slightly higher, which could have been expected.

To the best of our knowledge, the only report found to treat the influence of geometric characteristics of a spike is by Daniels and Yoshihara (see Ref. 2). They analyzed two types of spike, with flat and conical tips, and with length  $l > 1.5d$ , for  $M = 2.5$ . Therefore, a quantitative comparison with our results is not possible. However, their conclusions that the spike with a flat tip (provoking a stronger leading shock wave appearing in front of the tip) had better aerody-

namics features than the spike with a conical tip, can be taken as a qualitative verification of our results.

## Conclusions

The Note has treated experimentally the influence of different shapes of spikes mounted on a hemispherical nose of a blunt body, in a supersonic flow. The experiments were performed in a small trisonic wind tunnel, with Mach number  $M = 1.89$  and Reynolds number  $Re_d = 0.38 \times 10^6$ , and for four different spikes, of the length equal to the body diameter. The angle of attack varied from  $-4$  to  $10$  deg. The measurements of the aerodynamic load of the model were carried out to obtain the drag and lift coefficients. It has been shown that the shape of the spike has an important influence on the aerodynamic characteristics of the model, but also that it diminishes with the increase of the angle of attack. Spike 4, with a hemispherical tip and a cylindrical body, has been found to have the better aerodynamic characteristics. For that spike, and for the angles of attack from  $0$  to  $10$  deg, the drag coefficient is reduced from  $40$  to  $15\%$  in comparison with the same model without a spike. The lift coefficient is increased from  $86$  to  $29\%$  for the angles of attack from  $2$  to  $10$  deg in comparison with the same model without a spike.

To explain the influence of the shape of the spike, visualization experiments were performed in the same wind tunnel, using the schlieren technique. It has been shown that, in the case of the spike with a hemispherical tip (the fourth one), the leading shock wave appearing at the tip is curved, separated, and stronger than the conical shock wave appearing at a sharper tip in the case of the other tested geometries. However, this implies that the following, second shock wave, appearing at the shoulder of the body, is stronger for the leading conical shock wave. The total loss of mechanical energy is, therefore, less for the curved and separated leading shock wave. This reasoning has led to a formulation of a simple yet reliable criterion for estimating aerodynamic effects of a spike by using visualization only. The greater the radial distance of the joint point of the leading and the secondary shock waves from the axis, the better the aerodynamic characteristics of the tested configuration are.

## Acknowledgments

This research was partially supported by the Technical Institute of the Yugoslav Army. The authors would like to thank Danilo Ćuk, Slavica Ristić, Aleksandar Vitić, and other members of the Institute who kindly contributed their time and expertise.

## References

- Koenig, K., Bridges, D. H., and Chapman, G. T., "Transonic Flow Modes of an Axisymmetric Blunt Body," *AIAA Journal*, Vol. 27, No. 9, 1989, pp. 1301, 1302.
- Chang, P. K., "Flow Separation on Thin Protruding Probes Placed in Front of Blunt Bodies at Supersonic/Hypersonic Speeds," *Separation of Flow*, 1st ed., Pergamon, Oxford, 1970, pp. 469-530.
- Krasnov, N. F., and Koshevoy, V. N., "Drag and Lift Control," *Control and Stabilization in Aerodynamics*, Supreme School, Moscow, 1978, pp. 383-394 (in Russian).
- Calarese, W., and Hankey, W. L., "Modes of Shock-Wave Oscillations on Spike-Tipped Bodies," *AIAA Journal*, Vol. 23, No. 2, 1985, pp. 185-192.
- Milićević, S. S., and Pavlović, M. D., "Supersonic Flow Around Blunt Bodies of Revolution with Spikes," Faculty of Mechanical Engineering, Technical Rept. TR-2002-01, Univ. of Belgrade, Belgrade, 2002.
- Bogdonoff, S. M., and Vas, I. E., "Preliminary Investigations of Spiked Bodies at Hypersonic Speeds," *Journal of the Aero/Space Sciences*, Vol. 26, No. 2, 1959, pp. 65-74.
- "Equations, Tables, and Charts for Compressible Flow," NACA Rept. 1135, 1953.